

Movable but not removable band degeneracies in a symmorphic crystalMariana Malard,^{1,2} Paulo Eduardo de Brito,¹ Stellan Östlund,² and Henrik Johannesson^{2,3}¹*Faculty of Planaltina, University of Brasilia, 70904-910, Brasilia-DF, Brazil*²*Department of Physics, University of Gothenburg, SE 412 96 Gothenburg, Sweden*³*Beijing Computational Science Research Center, Beijing 100094, China* (Received 24 April 2018; revised manuscript received 25 September 2018; published 17 October 2018)

Crossings of energy bands in solids that are not pinned at symmetry points in the Brillouin zone and yet cannot be removed by perturbations are thought to be conditioned on the presence of a nonsymmorphic symmetry. In this article we show that such band crossings can actually appear also in a symmorphic crystal. A study of a class of tight-binding multiband one-dimensional lattice models of spinful electrons reveals that chiral, time-reversal, and site-mirror symmetries are sufficient to produce such *movable but not removable* band degeneracies.

DOI: [10.1103/PhysRevB.98.165127](https://doi.org/10.1103/PhysRevB.98.165127)**I. INTRODUCTION**

Level crossings—the appearance of degeneracies in the spectrum of a Hamiltonian—underlie a variety of phenomena, from quantum phase transitions [1] to properties of topological semimetals [2]. The noncrossing rule by von Neumann and Wigner [3] here gets circumvented by the presence of one or several symmetries which inhibit level repulsion. When a level crossing occurs through tuning a control parameter, the resulting degeneracy is said to be *accidental*; else, if symmetry alone dictates the presence of the degeneracy, it is commonly called *symmetry enforced*.

Level crossings, or “nodes,” play a particularly important role in the theory of electronic band structures of solids [4]. Whereas the possibility of accidental band degeneracies was pointed out early on [5], only rather recently have their physical implications been more systematically investigated, leading to the discovery of Weyl semimetals [6,7]. Symmetry-enforced degeneracies, on the other hand, have long played a key role in band theory. Typically pinned at high-symmetry momenta in the Brillouin zone (BZ) [8], they form the “essential” degeneracies well known from textbooks [9]. A seemingly unique situation occurs in the presence of a nonsymmorphic symmetry, i.e., when the crystal is invariant under a point group transformation combined with a *nonprimitive* lattice translation [9]. In this case, the electronic bands form a connected net [10] and while the resulting nodes cannot be lifted by symmetry-preserving perturbations, their location can be moved in the BZ by the same perturbation, leading to the notion of *movable but not removable degeneracies*.

The degeneracies which emerge from nonsymmorphic symmetries have come to play a crucial role in the theory of Dirac [11,12] and nodal line [13] semimetals. It has recently been shown that they may appear also in other unconventional band structures, leading to nodal chains [14] and surface modes with “hourglass” dispersions [15]. The mobility of these nodes throughout the BZ—when unconstrained by other symmetries—suggests that their robustness against perturbations is linked to a global topological invariant [16,17]. This is different from the movable accidental nodes in Weyl semimetals which are endowed with only local topological protection

[6]. For extended discussions of symmetry-enforced nodal phenomena in semimetals, and also in unconventional superconductors, see Refs. [18,19].

Given the importance of symmetry-enforced and yet unpinned degeneracies, one may inquire whether similar level crossings can appear also in a symmorphic crystal, characterized by invariance under point group transformations and *primitive* lattice translations [9]. In this article we show that this is indeed possible. Specifically, we show that a pair of movable but not removable nodes exists in the multiband spectra of a class of symmorphic tight-binding chains of spinful electrons possessing chiral, time-reversal, and site-mirror symmetries. When perturbed, these nodes move symmetrically in the BZ, conspicuously making them akin to Weyl nodes [6], with the crucial difference that here they cannot be pairwise annihilated through a perturbation which respects the underlying symmetries. Relevant for applications, realizations of the investigated class of models may be engineered from a quantum wire supporting spin-orbit interactions of arbitrary strength. The fact that the symmorphic mirror symmetry enforces movable but not removable nodes already in one spatial dimension allows for a simple and transparent analysis. We shall build our argument starting from a chain of spinless fermions, and then show how our result emerges by bringing in spin.

II. SPINLESS CHAINS WITH CHIRAL, TIME-REVERSAL, AND INVERSION SYMMETRIES

Consider a translational invariant one-dimensional (1D) lattice with $r \in 2\mathbb{N}$ sites per unit cell, distributed between two sublattices, one formed out of the odd-labeled sites and the other from the even-labeled sites. The chain is populated by spinless fermions with nearest-neighbor hopping only. The $r \times r$ Bloch matrix describing the system in the spinor representation introduced in the Supplemental Material (SM) [20] has the general form

$$\mathcal{H}(k) = \begin{bmatrix} 0 & Q(k) \\ Q^\dagger(k) & 0 \end{bmatrix}, \quad (1)$$

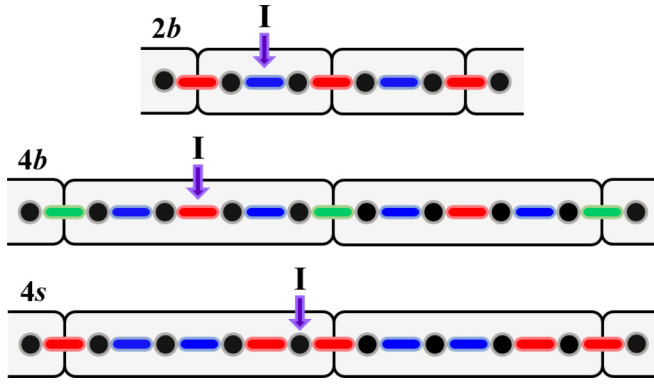


FIG. 1. Chains $2b$ and $4b$ with a bond-inversion point and chain $4s$ with a site-inversion point. The colored segments represent bonds with different strengths. The inversion point is indicated by I .

where $Q(k)$ is the matrix containing the hopping amplitudes between the two sublattices. The model supports chiral symmetry, i.e., $S\mathcal{H}(k)S^{-1} = -\mathcal{H}(k)$, with $S = \sigma_z \otimes \mathbb{1}_{r/2 \times r/2}$ the matrix implementing the chiral transformation. In addition, we impose time-reversal symmetry $\mathcal{T}\mathcal{H}(k)\mathcal{T}^{-1} = \mathcal{H}^*(-k)$ with $\mathcal{T} = \mathbb{1}_{r \times r}$, implying real hopping amplitudes, which we take to be positive.

There are two ways in which a tight-binding chain with nearest-neighbor hopping may be invariant under inversion. They differ by the inversion point being located on the bond between two sites—“bond inversion” or on a site—“site inversion.” Figure 1 illustrates both situations for $r = 2, 4$, with larger unit cells easily represented by repeating the underlying pattern. As seen in Fig. 1, a chain with two sites per unit cell supports only bond-inversion symmetry (chain $2b$), while for larger unit cells both types of symmetries are possible. Chain $2b$ corresponds to the well known spinless Su-Schrieffer-Heeger (SSH) model [21].

In the following we will analyze the cases with $r > 2$. Our goal is to establish the conditions under which the gap closes through the appearance of a zero-energy degeneracy. Given that chiral symmetry forces the spectrum of $\mathcal{H}(k)$ to be symmetric around zero energy [21], the existence of such a node is guaranteed if the spectrum has at least one zero eigenvalue. The latter requirement is fulfilled if $\det[Q(k)] = 0$. The Q matrices for the chains in Fig. 1 with $r = 4$ read

$$Q^{4b} = \begin{bmatrix} a & cz \\ b & a \end{bmatrix}, \quad Q^{4s} = \begin{bmatrix} a & bz \\ a & b \end{bmatrix}, \quad (2)$$

where $z = e^{-ik}$ with $k \in [-\pi, \pi]$, and a, b , and c are the hopping amplitudes along the blue, red, and green bonds, respectively [20]. The condition $\det[Q(k)] = 0$, subject to $|z| = 1$, implies in each case: $z = z^{4b} = a^2/(bc)$ if $a^2 = bc$; $z = z^{4s} = 1$ for any a and b . Since $z = e^{-ik}$, in both cases the node is located at $k = 0$, a consequence of a, b , and c being real numbers. The crucial difference comes from the constraint imposed on the hopping amplitudes, in the case of bond inversion, or lack thereof, in the case of site inversion: Bond-inversion symmetry, when combined with chiral and time-reversal symmetries, leads to an accidental node, while with site-inversion symmetry the degeneracy becomes

unavoidable. This conclusion immediately generalizes to a unit cell with $r > 4$ sites.

To prove that the combination of chiral (S), time-reversal (T), and site-inversion (I) symmetries enforces a $k = 0$ node, we consider the site-inversion transformation $I(k) = \mathcal{I}(k) \times \parallel$, where the “hard wall” operator \parallel reverses momentum and $\mathcal{I}(k)$ is an $r \times r$ matrix acting on the intracell positions,

$$\mathcal{I}(k) = \begin{bmatrix} R_1(k) & 0 \\ 0 & R_2(k) \end{bmatrix}. \quad (3)$$

The forms of the $R_1(k)$ and $R_2(k)$ matrices depend on the size of the unit cell. If $I(k)$ is a symmetry transformation, then $\mathcal{H}(k)$ must satisfy $\mathcal{I}(k)\mathcal{H}(-k)\mathcal{I}^{-1}(k) = \mathcal{H}(k)$ [20]. It follows, using Eqs. (1), (3), and the identity $\mathcal{I}^{-1}(k) = \mathcal{I}(-k)$, that $R_1(k)Q(-k)R_2(-k) = Q(k)$. With $r = 4$ sites per unit cell, $R_1(k) = z \text{adiag}(1, 1)$, $R_2(k) = z \text{diag}(1, z^*)$ [20], with the symbol diag (adiag) denoting a diagonal (antidiagonal) matrix and, as before, $z = e^{-ik}$. Assuming a generic $Q(k)$ with $r = 4$, it follows that the k -independent parameters appearing in $Q(k)$, call them q_{ij} , must satisfy $q_{21} = q_{11}$ and $q_{12} = q_{22}$. This confirms that Q^{4s} in Eq. (2) is the most general matrix describing a spinless STI -invariant chain with $r = 4$ sites per unit cell. Again, the procedure applies to an arbitrarily large unit cell with $r > 4$ once the corresponding $R_1(k)$ and $R_2(k)$ have been obtained [20].

One can now understand how the noncrossing rule is bypassed in the spinless STI -invariant chain. In order to avoid level repulsion, states must carry distinct quantum numbers. This requirement is satisfied by S which prescribes that degenerate zero-energy states are eigenstates of the chiral operator with opposite eigenvalues [21]. Still, S symmetry alone only paves the way for the appearance of an accidental degeneracy. Adding I symmetry constrains the Bloch matrix in such a way that a nodal solution exists in the whole parameter space. By enforcing real hopping amplitudes, T symmetry pins the node at $k = 0$. As we shall see, adding spin creates a pair of Kramers related nodes with the striking effect of unpinning them, without disrupting the symmetry enforcement.

A final remark on the spinless case: At a first glance, the k dependence of I might appear as a signature of a nonsymmorphic transformation, in which case our inversion would actually be a glide operation [9]. This is not the case: By the crystallographic definition, the k dependence of a nonsymmorphic transformation is along the direction parallel to the mirror plane [22]. In the case of a 1D system, k is, by construction, perpendicular to the plane of inversion. The k dependence of I instead comes about from the lack of invariance of the unit cell under the site-inversion transformation which, in turn, stems from the offset between the inversion point and the center of the cell (see Fig. 1). This is a feature of site inversion which does not occur with bond inversion. Using the property $\mathcal{I}(-k) = \mathcal{I}^{-1}(k)$, it can also be seen that $I^{2n}(k) = \mathbb{1}$, and thus $I^{2n+1}(k) = I(k)$, with $n = 1, 2, \dots$. This means that, unlike a nonsymmorphic transformation, $I(k)$ cannot be iterated to eventually produce a full translation $e^{ik}\mathbb{1}$. For discussions of other lattice models with symmorphic k -dependent symmetry transformations, see Refs. [23–25].

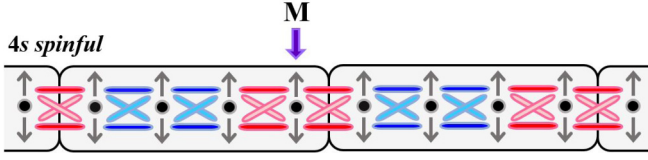


FIG. 2. The $4s$ -chain populated by spinful fermions. The colored segments represent bonds with different strengths; up and down arrows illustrate the spin degree of freedom. A site-mirror point is indicated by M .

III. SPINFUL CHAIN WITH CHIRAL, TIME REVERSAL, AND SITE-MIRROR SYMMETRIES

Let us consider again the minimal $4s$ chain which, in the spinful case, can be represented as in Fig. 2. The matrix Q^{4s} from Eq. (2) is now replaced by

$$\tilde{Q}^{4s} = \begin{bmatrix} A & B^* z \\ A^* & B \end{bmatrix}, \quad (4)$$

where the hopping amplitudes a and b became 2×2 matrices A and B whose diagonal (off-diagonal) entries account for hoppings with equal (flipped) spin [20]. An experimental realization of both the spin-conserving and spin-flipping terms in \tilde{Q}^{4s} may be found in a quantum wire with spatially modulated Rashba and uniform Dresselhaus spin-orbit interactions [26]. The Bloch matrix, given by Eq. (1), supports S symmetry with $S = \sigma_z \otimes \mathbb{1}_{r \times r}$. With $T = \mathbb{1}_{r \times r} \otimes (-i\sigma_y)$ now being the matrix which implements a spin flip, T symmetry is fulfilled if $(-i\sigma_y)X(i\sigma_y) = X^*$, $X = A, B$. Applying this relation to A and B , we get $x_{22} = x_{11}^*$, $x_{21} = -x_{12}^*$, $x = a, b$. These constraints replace the stronger condition of real hopping amplitudes imposed by T in the spinless case, resulting in unpinned band degeneracies.

To see this, let us remove T and consider \tilde{Q}^{4s} in Eq. (4), now with unconstrained A and B . For general A and B , $\det[\tilde{Q}^{4s}] = p^* z^2 + qz + p$, where

$$\begin{aligned} p &= \det A \det B = |p| e^{i\alpha}, \\ q &= 2 \sum_{x \neq y} \text{Re}(x_{11} x_{22}^* y_{12} y_{21}^*) - 2 \text{Re}(a_{11} a_{22}^* b_{11} b_{22}^*) \\ &\quad - 2 \text{Re}(a_{12} a_{21}^* b_{12} b_{21}^*) - 4 \sum_{x \neq y} \text{Im}(x_{11} x_{12}^*) \text{Im}(y_{21} y_{22}^*), \end{aligned} \quad (5)$$

with $x, y = a, b$. The condition $\det[Q(k)] = 0$ yielding a zero-energy node is fulfilled if $z = z_{\pm} = (t \pm \sqrt{t^2 - 1}) e^{i\alpha}$, where $t \equiv -q/(2|p|)$. Since $|z_{\pm}| = 1$, one must have $t \in [-1, 1]$, in which case $z_{\pm} = e^{i(\pm\theta + \alpha)}$, with $\theta = \arctan(\sqrt{1 - t^2}/t)$ if $0 \leq t \leq 1$ or $\theta = \arctan(\sqrt{1 - t^2}/t) + \pi$ if $-1 \leq t < 0$. Therefore, a pair of nodes occurs at $k = k_{\pm} = \pm\theta + \alpha$ and they move (asymmetrically with respect to $k = 0$) as the phases θ and α change. It follows from the definition of t and Eqs. (5) that satisfying $t \in [-1, 1]$ demands fine tuning the microscopic parameters, meaning that such a node would be accidental. These nodes are shown in a movie appended to the SM [20].

We now reintroduce the T -constraints $x_{22} = x_{11}^*$, $x_{21} = -x_{12}^*$, $x = a, b$, for which p in Eq. (5) becomes a real positive

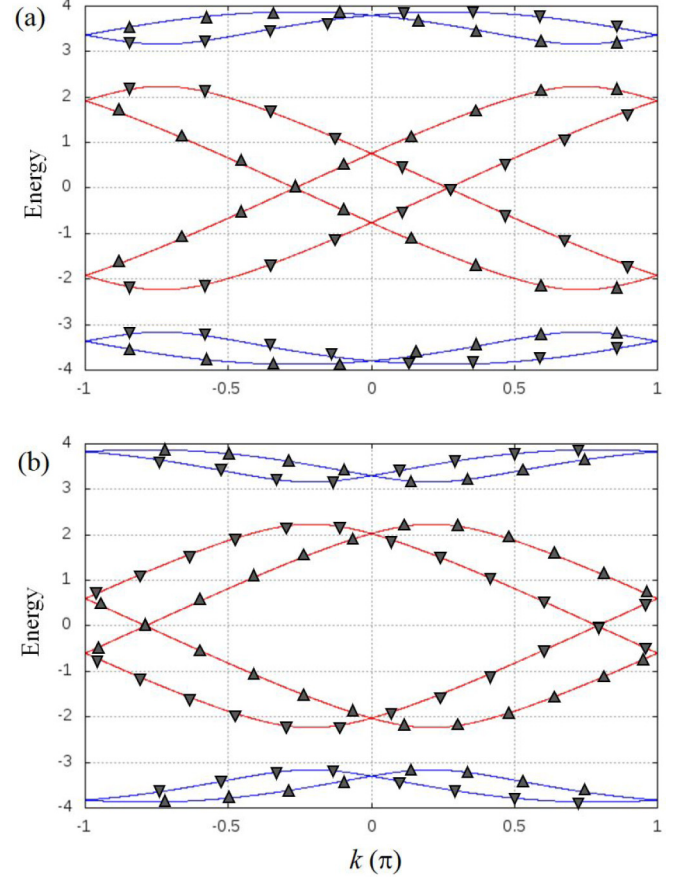


FIG. 3. Spectrum of the spinful $4s$ chain for (a) $\theta_{a_{11}} = 1.53\pi$ and (b) $\theta_{a_{11}} = 0.04\pi$. For both (a) and (b): $|a_{11}| = 2$, $|a_{12}| = 1$, $|b_{11}| = \sqrt{2}/2$, $|b_{12}| = \sqrt{2}$, and $\theta_{a_{12}} = \pi/6$, $\theta_{b_{11}} = \pi/3$, $\theta_{b_{12}} = \pi/12$. Color code: Red and blue are employed on the bands to highlight the symmetry of the spectrum around energy = 0 and $k = 0$, a consequence of chiral and time-reversal symmetries, respectively. Up and down triangles represent the two opposite spin orientations.

number, i.e., $\alpha = 0$, $|p| = p$. Also, under the T constraints $t \in (-1, 1)$, and hence $|z_{\pm}| = 1$ with no further constraints on the parameters. It follows that $z_{\pm} = e^{\pm i\theta}$ meaning that two nodes occur at the BZ points $k = k_{\pm} = \pm\theta$, with θ as given above but excluding $t = \pm 1$. The effect of T is thus to turn the former asymmetric pair of accidental nodes into a symmetric pair of *movable but not removable* degeneracies. Figure 3 illustrates the spectrum for two parameter configurations, with the parameters x_{ij} , $x = a, b$, written as $x_{ij} = |x_{ij}| \exp(i\theta_{x_{ij}})$. At the node for positive (negative) k , the two degenerate states have both spin down (up), so the four zero-energy states together form two Kramers pairs. In the SM [20] the reader will find movies of the spectrum which fully exposes the motion of the nodes in the BZ for different parameter variations.

The BZ locations of the nodes, given by $k_{\pm} = \pm\theta$, are shown in Fig. 4 as a function of the phase and of the modulus of a_{11} . Figure 4(a) shows that as $\theta_{a_{11}}$ goes from 0 to 2π , the nodes at opposite sides of the BZ bounce back and forth between the center and the zone boundaries. Varying $|a_{11}|$ causes the nodes to initially approach each other, but they

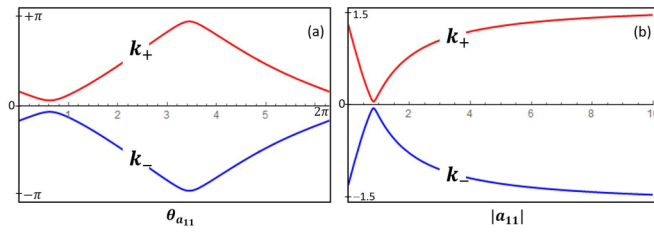


FIG. 4. The locations k_{\pm} of the nodes as a function of (a) $\theta_{a_{11}}$ with $|a_{11}| = 1$ and (b) $|a_{11}|$ with $\theta_{a_{11}} = \pi/5$. For both (a) and (b): $|a_{12}| = |b_{11}| = |b_{12}| = 1$ and $\theta_{a_{12}} = 5\pi/8$, $\theta_{b_{11}} = 2\pi/3$, $\theta_{b_{12}} = \pi/4$.

are eventually pushed apart, as shown in Fig. 4(b). In neither case do the nodes merge at $k = 0$ or at $k = \pm\pi$. Mathematically, this fact follows from z_{\pm} being complex numbers, hence $z_{\pm} \neq \pm 1$ and thus $k_{\pm} \neq 0, \pm\pi$. Differently from the Weyl nodes [6] and the triple point fermions discussed in Ref. [27] (which, in both cases, are topologically protected only locally), our symmetry-enforced nodes cannot coalesce and annihilate. However, the effective repulsion between the nodes as they symmetrically approach the center or the boundaries of the BZ is not easily explained by symmetry alone. Topology may conceivably also play a role, similar to the case of nonsymmorphic degeneracies which come with a global topological invariant [17].

To conclude our analysis, we show that the form of \tilde{Q}^{4s} in Eq. (4) follows from the combination of T and a site-mirror (M) symmetries. For that we construct the unitary site-mirror transformation $M(k) = I(k)\mathcal{T}$ formed out of site-inversion $I(k) = \tilde{\mathcal{I}}(k) \times \parallel$ times the spin flip \mathcal{T} . For the spinful chain, $\tilde{\mathcal{I}}(k) = \mathcal{I}(k) \otimes \mathbb{1}_{2 \times 2}$. Employing Eq. (3),

$$\mathcal{M}(k) \equiv \tilde{\mathcal{I}}(k)\mathcal{T} = \begin{bmatrix} \tilde{R}_1(k) & 0 \\ 0 & \tilde{R}_2(k) \end{bmatrix}, \quad (6)$$

with $\tilde{R}_1(k) = R_1(k) \otimes (-i\sigma_y)$ and $\tilde{R}_2(k) = R_2(k) \otimes (-i\sigma_y)$. Demanding that $M(k)$ is a symmetry transformation yields $\mathcal{M}(k)\mathcal{H}(-k)\mathcal{M}^{-1}(k) = \mathcal{H}(k)$ [20]. Bringing in Eqs. (1) and (6), and using that $\mathcal{M}^{-1}(k) = -\mathcal{M}(-k)$, it follows that $\tilde{R}_1(k)Q(-k)\tilde{R}_2(-k) = -Q(k)$. Inserting a generic $Q(k)$ with $r = 4$ into this relation leads to $(-i\sigma_y)Q_{ij}(i\sigma_y) = Q_{jj}$, with $i \neq j = 1, 2$, and Q_{ij} the k -independent 2×2 matrices appearing in $Q(k)$. Combining this with the fact that T constrains these matrices as $(-i\sigma_y)Q_{ij}(i\sigma_y) = Q_{ij}^*$, we get $Q_{ij} = Q_{jj}^*$, with $i \neq j = 1, 2$. This means that \tilde{Q}^{4s} in Eq. (4) is indeed the most general matrix describing a spinful STM -invariant chain with $r = 4$ sites per unit cell. The analysis can

be extended to unit cells with $r > 4$, and one concludes that any spinful STM -invariant chain exhibits a pair of movable but not removable degeneracies.

IV. SYMMETRY CLASSES

Let us briefly discuss the symmetry classes of the studied models. In the presence of S and T symmetries, the multiband spinless (spinful) chain belongs to class BDI (CII) [20] of the Altland-Zirnbauer classification [28]. This means that the spinless STI - and the spinful STM -invariant chains are at the boundary between trivial and topological insulating phases which, in both cases, can be characterized by a Z -winding number. Breaking the I or M symmetry will generically open a gap at zero energy, driving the system into either one of the insulating regimes. This is similar to how a nonsymmorphic symmetry correlates with a topological phase transition in models of 2D Dirac semimetals [12].

V. SUMMARY

We have identified a class of 1D electronic tight-binding models which allow the presence of spin-orbit interactions and whose band structures exhibit *movable but not removable* degeneracies without the presence of a nonsymmorphic symmetry. Chiral, time-reversal, and site-mirror symmetry comprise a sufficient set of symmetries for the emergence of this type of degeneracy which, in the case at hand, come in the form of a Kramers related pair of nodes. An interesting open problem is whether these nodes are endowed with a global topological invariant, analogous to the case of nonsymmorphic degeneracies [17]. Possible generalizations include adding longer-range odd-neighbor hoppings or superconducting pairing that preserve the enforcing symmetries. Of obvious interest would be to extend our finding to higher dimensions. This could open a pathway to search for new nodal semimetals in symmorphic crystals and, important for applications, in the presence of strong spin-orbit interactions.

ACKNOWLEDGMENTS

It is a pleasure to thank Jens Bardarson, Jan Budich, Maria Hermanns, Gia Japaridze, Andreas Schnyder, Alexander Stolin, and Long Zhang for valuable discussions. This research was supported by the Swedish Research Council (Grant No. 621-2014-5972).

[1] S. Sachdev, *Quantum Phase Transitions* (Cambridge University Press, Cambridge, 2001).
 [2] N. P. Armitage, E. J. Mele, and A. Vishwanath, *Rev. Mod. Phys.* **90**, 015001 (2018).
 [3] J. von Neumann and E. Wigner, *Phys. Z.* **30**, 465 (1929).
 [4] R. M. Martin, *Electronic Structure: Basic Theory and Practical Methods* (Cambridge University Press, Cambridge, 2004).
 [5] C. Herring, *Phys. Rev.* **52**, 365 (1937).
 [6] S. Murakami, *New J. Phys.* **9**, 356 (2007).

[7] X. Wan, A. M. Turner, A. Vishwanath, and S. Y. Savrasov, *Phys. Rev. B* **83**, 205101 (2011).
 [8] L. P. Bouckaert, R. Smoluchowski, and E. Wigner, *Phys. Rev.* **50**, 58 (1936).
 [9] M. S. Dresselhaus, G. Dresselhaus, and A. Jorio, *Group Theory: Applications to the Physics of Condensed Matter* (Springer, Berlin, 2008).
 [10] L. Michel and J. Zak, *Phys. Rev. B* **59**, 5998 (1999).
 [11] S. M. Young, S. Zaheer, J. C. Y. Teo, C. L. Kane, E. J. Mele, and A. M. Rappe, *Phys. Rev. Lett.* **108**, 140405 (2012).

- [12] S. M. Young and C. L. Kane, *Phys. Rev. Lett.* **115**, 126803 (2015).
- [13] C. Fang, Y. Chen, H.-Y. Kee, and L. Fu, *Phys. Rev. B* **92**, 081201(R) (2015).
- [14] T. Bzdusek, Q. S. Wu, A. Rüegg, M. Sigrist, and A. A. Soluyanov, *Nature (London)* **538**, 75 (2016).
- [15] Z. Wang, A. Alexandradinata, R. J. Cava, and B. A. Bernevig, *Nature (London)* **532**, 189 (2016).
- [16] J. Zak, *J. Phys. A* **35**, 6509 (2002).
- [17] Y. X. Zhao and Andreas P. Schnyder, *Phys. Rev. B* **94**, 195109 (2016).
- [18] H. Watanabe, H. C. Po, M. P. Zaletel, and A. Vishwanath, *Phys. Rev. Lett.* **117**, 096404 (2016); B. J. Wieder, Y. Kim, A. M. Rappe, and C. L. Kane, *ibid.* **116**, 186402 (2016); B. J. Wieder and C. L. Kane, *Phys. Rev. B* **94**, 155108 (2016); S. M. Young and B. J. Wieder, *Phys. Rev. Lett.* **118**, 186401 (2017); J. Wang, *Phys. Rev. B* **95**, 115138 (2017).
- [19] T. Micklitz and M. R. Norman, *Phys. Rev. B* **95**, 024508 (2017); *Phys. Rev. Lett.* **118**, 207001 (2017); T. Nomoto and H. Ikeda, *J. Phys. Soc. Jpn.* **86**, 023703 (2017); S. Kobayashi, S. Sumita, Y. Yanase, and M. Sato, *Phys. Rev. B* **97**, 180504(R) (2018); W. Brzezicki and M. Cuoco, *ibid.* **97**, 064513 (2018).
- [20] See Supplemental Material at <http://link.aps.org/supplemental/10.1103/PhysRevB.98.165127> for details of the formalism and movies of the band structure.
- [21] J. K. Asbóth, L. Oroszlány, and A. Pályi, *A Short Course on Topological Insulators* (Springer, Berlin, 2016).
- [22] A. König and N. D. Mermin, *Phys. Rev. B* **56**, 13607 (1997).
- [23] B.-J. Yang, T. A. Bojesen, T. Morimoto, and A. Furusaki, *Phys. Rev. B* **95**, 075135 (2017).
- [24] J. Zhang, Y.-H. Chan, C.-K. Chiu, M. G. Vergniory, L. M. Schoop, and A. P. Schnyder, *Phys. Rev. Mater.* **2**, 074201 (2018).
- [25] W. Brzezicki and M. Cuoco, *Phys. Rev. B* **95**, 155108 (2017).
- [26] M. Malard, G. I. Japaridze, and H. Johannesson, *Phys. Rev. B* **94**, 115128 (2016).
- [27] I. C. Fulga and A. Stern, *Phys. Rev. B* **95**, 241116(R) (2017).
- [28] C.-K. Chiu, J. C. Y. Teo, A. P. Schnyder, and S. Ryu, *Rev. Mod. Phys.* **88**, 035005 (2016).